

Raman spectroscopy sheds new light on TiC formation during the controlled milling of titanium and carbon

B.H. Lohse, A. Calka*, D. Wexler

Faculty of Engineering, University of Wollongong, Northfields Avenue, Wollongong, NSW 2522, Australia

Available online 17 October 2006

Abstract

A magneto ball mill was used to mill titanium and carbon elemental powder mixtures with compositions of $\text{Ti}_{50}\text{C}_{50}$ and $\text{Ti}_{60}\text{C}_{40}$ under a helium atmosphere. Previous studies on the milling of titanium and carbon powder mixtures have reported a sudden increase in the temperature of the milling vial, which occurs after a specific milling interval, referred to as t_{ig} [Z.G. Liu, J.T. Guo, L.L. Ye, G.S. Li, Z.Q. Hu, Appl. Phys. Lett. 65 (1994) 2666–2668; G.B. Schaffer, J.S. Forrester, J. Mater. Sci. 32 (1997) 3157–3162; N.Q. Wu, S. Lin, J.M. Wu, Z.Z. Li, Mater. Sci. Technol. 14 (1998) 287–291; Z. Xinkun, Z. Kunyu, C. Baochang, L. Qiushi, Z. Xiuqin, C. Tieli, S. Yunsheng, Mater. Sci. Eng. C 16 (2001) 103–105; C. Deidda, S. Doppiu, M. Monagheddu, G. Cocco, J. Metastable Nanocryst. Mater. 15/16 (2003) 215–220]. This sudden temperature increase has been found to correspond to the formation of TiC via a rapid, highly exothermic reaction. In these cases, XRD analysis did not detect TiC in powder sampled before t_{ig} . These results, combined with those from studies suggested that the milling period prior to t_{ig} represents an incubation period during which the powders become mechanically activated and that no reaction between the starting powders occurs during this time [L. Takacs, J. Solid State Chem. 125 (1996) 75–84; B.K. Yen, T. Aizawa, J. Kihara, J. Am. Ceram. Soc. 81 (1998) 1953–1956; M. Puttaswamy, Y. Chen, B. Jar, J.S. Williams, Mater. Sci. Forum 312–314 (1999) 79–84; G.B. Schaffer, P.G. McCormick, Metall. Transact. A 23A (1992) 1285–1290; M. Mingliang, L. Xinkuan, X. Shenqui, C. Donglang, Z. Jingen, J. Mater. Process. Technol. 116 (2001) 124–127].

In the current investigation a sudden increase in the temperature of the milling vial was also observed after a specific milling duration of t_{ig} . XRD analysis of powder sampled before t_{ig} did not detect TiC, whilst for powder sampled after t_{ig} , XRD analysis indicated that the powder had almost completely transformed into TiC. However, Raman spectroscopy showed the formation of non-stoichiometric TiC in $\text{Ti}_{50}\text{C}_{50}$ and $\text{Ti}_{60}\text{C}_{40}$ powders sampled before t_{ig} . It is believed that the current, and many previous XRD analyses did not detect the formation of TiC prior to t_{ig} either because the TiC grain size was too small and/or the phase represented too small a volume fraction of the powder samples to be detected by the XRD method employed. These Raman spectroscopy results suggest that a significant component of the heat generated at t_{ig} may be due to a combination of growth of TiC accompanied by consumption of unreacted Ti and carbon, and/or recrystallisation of the TiC formed prior to t_{ig} , rather than the direct formation of TiC.

© 2006 Elsevier B.V. All rights reserved.

Keywords: Nanostructured materials; High-energy ball milling; Mechanochemical synthesis

1. Introduction

Titanium carbide (TiC) is suited to a number of commercial applications, such as abrasives, cutting tools, grinding wheels and coated cutting tips because it exhibits very high hardness, high melting temperature and excellent thermal and chemical stability [1,11–14]. Recent studies have shown that high-energy milling of titanium and carbon powders may be a viable synthesis method for the production of TiC powder [1–6,12–16].

However, the process by which titanium and carbon react to form TiC during milling is not yet well understood. The aim of this study is to further the understanding of this reaction through the use of Raman spectroscopy to characterise the milling products.

Very little has been reported on the use of Raman spectroscopy to study TiC. The literature states that stoichiometric TiC has no Raman active vibrational modes and that Raman scattering in TiC is due to disorder induced by carbon vacancies [17,18]. Klein et al. [17] produced Raman spectra of TiC_x where $x = 0.97, 0.90$ and 0.80 , whilst Amer et al. [18] published a Raman spectrum of $\text{TiC}_{0.67}$.

* Corresponding author. Tel.: +61 2 4221 4945; fax: +61 2 4221 3112.
E-mail address: acalka@uow.edu.au (A. Calka).

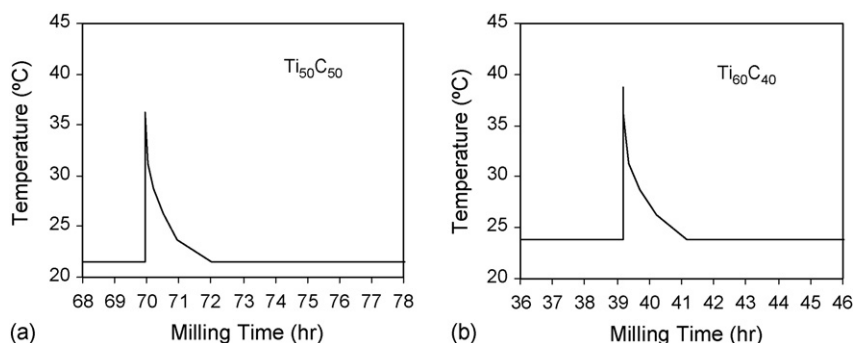


Fig. 1. Temperature of the milling vial during milling of titanium and carbon.

2. Experimental

Titanium powder of particle size $<250\ \mu\text{m}$ and minimum purity of 99.9% was mixed with high purity activated carbon powder to give compositions of $\text{Ti}_{50}\text{C}_{50}$ and $\text{Ti}_{60}\text{C}_{40}$. Controlled ball milling was performed using a magento ball mill (Uni-Ball-Mill 5) operating in impact mode under a high purity helium atmosphere. Samples were taken using a glovebag to prevent contamination of the powders. The external temperature of the milling vial was monitored during milling using an infrared thermometer.

X-ray diffraction (XRD) analysis of the as-milled powders was performed using a Phillips PW1730 diffractometer with $\text{Cu K}\alpha$ radiation. Raman spectroscopy was performed using a Jobin Yvon HR800 confocal Raman with a $632.8\ \text{nm}$ laser. The Raman spectra were recorded in the range between 200 and $1800\ \text{cm}^{-1}$ with an acquisition time of $50 \times 5\ \text{s}$. Spectra were taken from at least five different particles so as to examine the homogeneity of the powder.

3. Results

3.1. XRD analysis of as-milled Ti–C powders

An abrupt increase in the temperature of the milling vial was observed after milling for a specific duration, referred to as the ignition time, t_{ig} . The average ignition time for $\text{Ti}_{50}\text{C}_{50}$ was approximately 71 h, whilst that for $\text{Ti}_{60}\text{C}_{40}$ was approximately 41 h. Typical plots of the milling vial temperature versus milling time are shown in Fig. 1. The ignition time was repeatable within $\pm 2\ \text{h}$ of the average ignition time.

The XRD patterns for samples taken before and after t_{ig} are shown in Figs. 2 and 3 for $\text{Ti}_{50}\text{C}_{50}$ and $\text{Ti}_{60}\text{C}_{40}$, respectively.

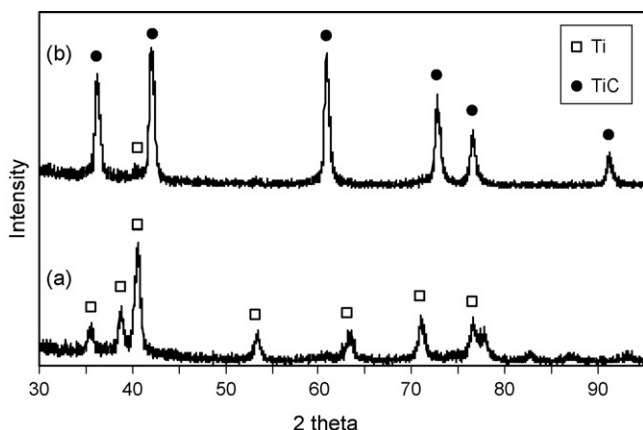


Fig. 2. XRD patterns for $\text{Ti}_{50}\text{C}_{50}$ after milling for (a) 66 h; (b) 82 h.

The XRD patterns for both compositions display only broad peaks corresponding to titanium before t_{ig} (Figs. 2(a) and 3(a)). After t_{ig} the XRD patterns for both $\text{Ti}_{50}\text{C}_{50}$ and $\text{Ti}_{60}\text{C}_{40}$ contain strong TiC peaks and a very weak peak at approximately 40° corresponding to unreacted titanium; indicating that the powder has almost completely transformed into TiC.

3.2. Raman spectroscopy of as-received Ti, C and TiC

The titanium starting powder did not produce a Raman spectrum, indicating that titanium does not have Raman active vibrational modes, at least for the spectral range recorded in this study. The Raman spectra for the activated carbon starting powder, shown in Fig. 4, display two strong peaks at approximately 1320 and $1590\ \text{cm}^{-1}$, which are associated with the A_{1g} and E_{2g} vibrational modes of graphite [18]. The Raman spectra for Aldrich[®] TiC powder with a purity of 98% are shown in Fig. 5. These spectra show two broad peaks that correspond to graphite, indicating the presence of some unreacted carbon in the commercial TiC powder. There are also three peaks at approximately 260 , 420 and $605\ \text{cm}^{-1}$, which are comparable to those reported by Klein et al. [17] and Amer et al. [18]. The spectra for the commercial TiC powder exhibit a range of different peak intensities and overall have much lower intensities than the peaks in the spectra of the carbon starting powder. A possible explanation for the low peak intensities is that the bulk of the material may be stoichiometric TiC, which has no Raman

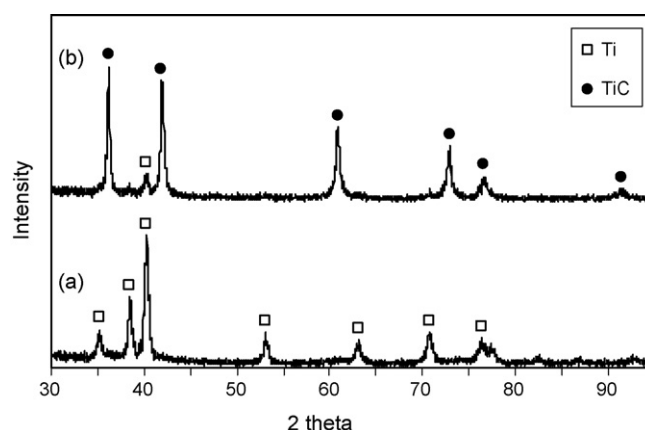


Fig. 3. XRD patterns for $\text{Ti}_{60}\text{C}_{40}$ after milling for (a) 36 h; (b) 60 h.

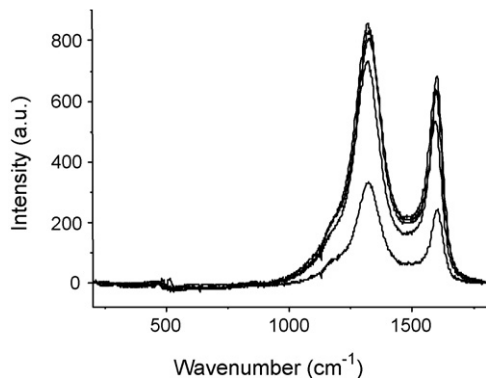


Fig. 4. Raman spectra of as-received TiC powder.

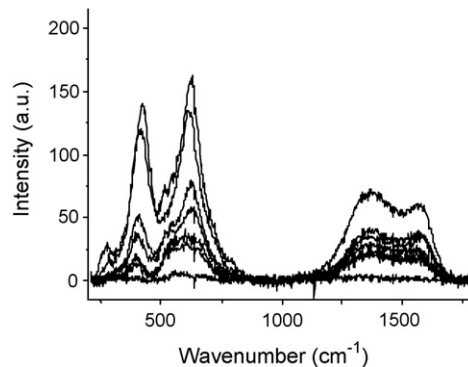


Fig. 5. Raman spectra of commercial activated carbon.

active vibrational modes, and so would not produce a Raman spectrum.

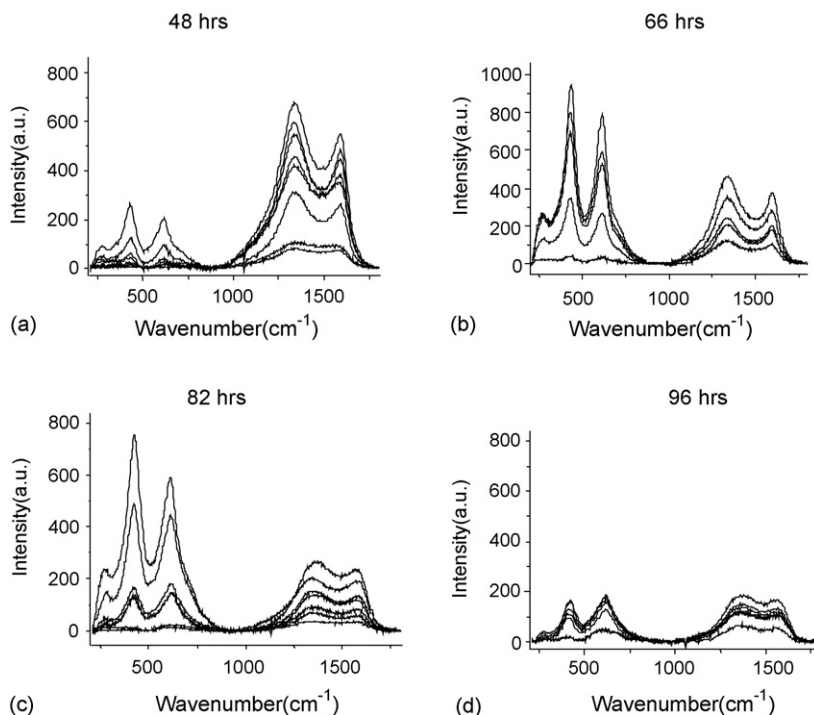
3.3. Raman spectroscopy of as-milled Ti–C powders

Fig. 6(a) shows the Raman spectra for $\text{Ti}_{50}\text{C}_{50}$ after milling for 48 h. XRD analysis of this powder revealed only peaks corresponding to titanium. However, the Raman spectra show strong graphite peaks at approximately 1320 and 1590 cm^{-1} and also weak peaks at approximately 260 , 420 and 605 cm^{-1} that correspond to TiC. The Raman spectra of $\text{Ti}_{50}\text{C}_{50}$ after milling for 48 h also show considerable variation in the relative intensities of the TiC and carbon peaks. This is most likely because the powder is still quite inhomogeneous at this early stage of milling.

The Raman spectra for $\text{Ti}_{50}\text{C}_{50}$, sampled after milling for 66 h, are shown in Fig. 6(b). XRD analysis of this powder revealed only peaks corresponding to titanium. However, the

Raman spectra display strong peaks corresponding to TiC and also broad graphite peaks. Compared to the spectra obtained after milling for 48 h, the intensity of the TiC peaks relative to the intensity of the graphite peaks has increased greatly; suggesting an increase in the amount of TiC present in the powder and a reduction in the amount of unreacted carbon as a result of further milling.

The Raman spectra for $\text{Ti}_{50}\text{C}_{50}$, sampled after milling for 82 h, are shown in Fig. 6(c). XRD analysis of this powder revealed strong peaks corresponding to TiC and a very weak peak corresponding to a little unreacted titanium. The Raman spectra show TiC and graphite peaks. The graphite peaks are much broader and less intense than the TiC peaks in the spectra shown in Fig. 6(a) and (b). This is most likely because the XRD results indicate that the bulk of the powder has reacted to form TiC and therefore contains far less unreacted carbon. Some of the spectra in Fig. 6(c) show only very broad, weak

Fig. 6. Raman spectra of $\text{Ti}_{50}\text{C}_{50}$ milled for (a) 48 h; (b) 66 h; (c) 82 h; (d) 96 h.

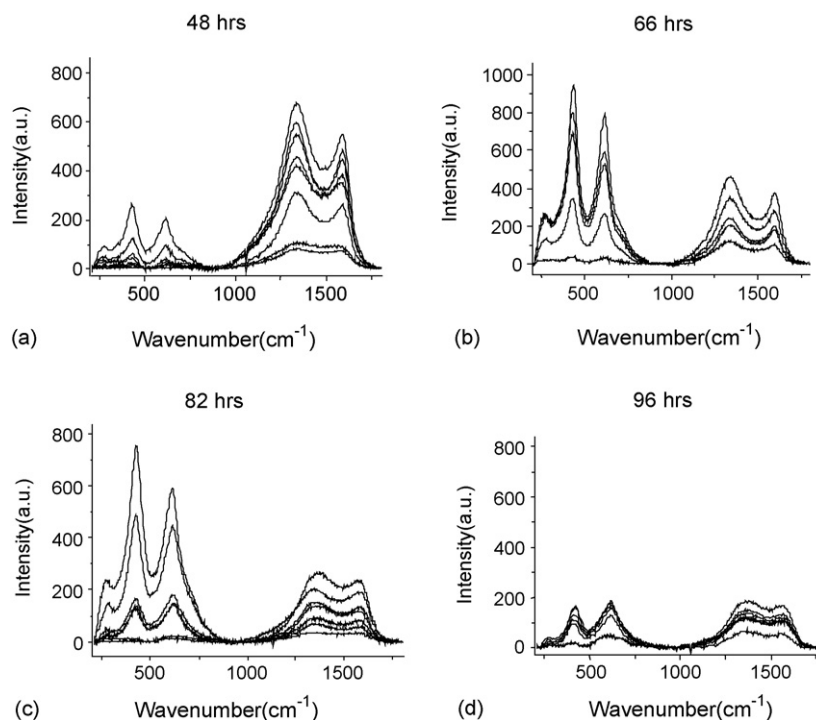


Fig. 7. Raman spectra of $\text{Ti}_{60}\text{C}_{40}$ milled for (a) 24 h; (b) 36 h; (c) 60 h; (d) 73 h.

peaks. This may indicate that these areas consist mainly of stoichiometric TiC, which does not produce a Raman spectrum.

Fig. 6(d) shows the effect of further milling on the Raman spectra of the $\text{Ti}_{50}\text{C}_{50}$ powder. In this figure are the spectra for $\text{Ti}_{50}\text{C}_{50}$ after milling for 96 h. Further milling results in further broadening of the Raman peaks and a reduction in peak intensity, particularly for the TiC peaks. This is thought to be due to unreacted carbon reacting with non-stoichiometric TiC to form stoichiometric TiC as milling continues. Because only unreacted carbon and non-stoichiometric TiC are Raman active, as the reaction progresses during further milling to produce stoichiometric TiC, which does not produce a Raman spectrum, the intensity of the Raman peaks decrease with further milling.

Fig. 7(a) and (b) shows the Raman spectra for $\text{Ti}_{60}\text{C}_{40}$ after milling for 24 and 36 h, respectively. XRD analysis of these powders revealed only titanium peaks. The ignition time (t_{ig}) for $\text{Ti}_{60}\text{C}_{40}$ was approximately 41 h. However, the Raman spectra for $\text{Ti}_{60}\text{C}_{40}$ display peaks corresponding to TiC after milling for only 24 h. After milling for 36 h, the intensity of the TiC peaks has increased whilst the intensity of the graphite peaks has decreased; indicating an increase in the amount of TiC present and a corresponding decrease in the amount of unreacted carbon. Both figures show considerable variation in the intensities of the TiC peaks relative to the graphite peaks; suggesting that the powders are far from homogeneous.

The Raman spectra shown in Fig. 7(c) and (d) are of $\text{Ti}_{60}\text{C}_{40}$ sampled after t_{ig} , with milling times of 60 and 73 h, respectively. XRD analysis of both of these samples revealed strong TiC peaks and a very weak peak corresponding to some unreacted titanium. The Raman spectra both show peaks corresponding to graphite; indicating that some unreacted carbon still remains. Comparing

the two sets of spectra reveal that both the TiC and graphite peaks weaken with further milling, which is most likely due to further milling resulting in some of the unreacted carbon reacting with non-stoichiometric TiC to form stoichiometric TiC. If standard samples were deliberately made up of blended non-stoichiometric and stoichiometric nanostructural TiC it may be possible to obtain quantitative estimates of the amount of non-stoichiometric TiC in the current milled materials prior to t_{ig} . However, due to the complex nanostructural nature of the product and complexities of analysis of TiC and graphite Raman peaks such an investigation would require very careful interpretation.

4. Discussion

When milling $\text{Ti}_{50}\text{C}_{50}$ and $\text{Ti}_{60}\text{C}_{40}$ elemental powder mixtures, a sudden increase in the temperature of the milling vial was observed after a milling duration of t_{ig} . XRD analysis of powder sampled before t_{ig} revealed only peaks corresponding to titanium. For powder sampled after t_{ig} , XRD analysis revealed strong peaks corresponding to TiC and a very weak peak corresponding to a small amount of unreacted titanium. These results suggest that the sudden temperature increase detected during milling is due to the rapid exothermic reaction to form TiC. This type of abrupt exothermic reaction taking place during milling has been referred to as a mechanically induced self-propagating reaction (MSR) [7].

Previous studies of mechanically induced self-propagating reactions have described the milling period before t_{ig} as simply an incubation or activation period [1,6–10,16]. Milling during this incubation period results in reductions in particle and

crystallite sizes and intimate mixing of the reactants, which results in an increase in the reaction interfacial area, combined with an accumulation of defects in the powder particles; all of which is thought to result in a reduction in the activation barrier for the reaction. It was thought that no reaction takes place until t_{ig} , when ignition occurs, and the reaction then continues as a self-propagating reaction.

The above XRD results for $Ti_{50}C_{50}$ and $Ti_{60}C_{40}$ elemental powder mixtures, showing only peaks corresponding to titanium before t_{ig} and TiC peaks after t_{ig} , suggest that for these systems, TiC is formed via a typical mechanically induced self-propagating reaction. However, the Raman results clearly show the formation of TiC well before t_{ig} . The fact that XRD analysis did not detect the formation of TiC before t_{ig} suggests that the grain size of the TiC detected by Raman spectroscopy is too small and/or the volume fraction of this phase is too small to be detected using the XRD method employed in this study.

Raman spectroscopy clearly shows the formation of non-stoichiometric TiC prior to t_{ig} . Such material, either in the form of small crystals or crystal nuclei, represents likely nucleation points for subsequent rapid transformation following further mechanical deformation. Rather than a single step nucleation and growth process a two step process appears likely. It is now thought that a significant component of the heat generated at t_{ig} is due to some combination of rapid grain growth from pre-existing nuclei of non-stoichiometric TiC and/or recrystallisation of TiC from pre-existing crystallites followed by further rapid grain growth and transformation to predominately stoichiometric product. During this rapid exothermic growth stage, occurring at around t_{ig} , both unreacted carbon and the large amount of unreacted nanostructural titanium combine to form stoichiometric TiC.

Such a two stem mechanism involving nucleation during earlier stages of milling and rapid exothermal growth at some latter stage is contrary to the existing understanding of MSR, which is based on studies that have used only XRD analysis to characterise as-milled powders [1,6–10,16]. In these studies, no reaction product was detected prior to t_{ig} , and the heat generated at t_{ig} was thought to be entirely due to the exothermic reaction to form the new reaction product. Further work is required to determine whether the formation of reaction product prior to t_{ig} is unique to this system, or if it occurs during milling in other systems where MSR occurs but has simply gone undetected.

5. Conclusions

Raman spectroscopy detected the formation of TiC well before it was detected by XRD analysis. For $Ti_{50}C_{50}$ and $Ti_{60}C_{40}$ elemental powder mixtures, the combined results of external mill temperature monitoring and X-ray diffractometry indicated that, after a milling duration of t_{ig} , TiC formed rapidly via a mechanically induced reaction which resulted in sudden heat-

ing of the milling vial. However, Raman spectroscopy clearly showed the formation of non-stoichiometric TiC prior to t_{ig} . This is a result not reported in studies that have used only XRD analysis to characterise the as-milled powders. These results suggest that a significant component of the heat generated at t_{ig} may be due to a combination of rapid grain growth and/or recrystallisation of the TiC formed prior to t_{ig} , rather than the direct formation of TiC. Raman spectroscopy also indicated that the amounts of both non-stoichiometric TiC and unreacted carbon decreased with further milling after t_{ig} . This suggests that some of the unreacted carbon reacts with non-stoichiometric TiC to form stoichiometric TiC during further milling.

Acknowledgements

The authors wish to thank Dr. Peter Innis from the Intelligent Polymer Research Institute and ARC Centre for Nanostructured Electromaterials at the University of Wollongong for his help and advice with the Raman spectroscopy. The authors also gratefully acknowledge financial support from the Australian Research Council, under ARC-Large Grant No. A00103022 and ARC-Discovery Grant No. DP0451907. The Reviewer is also acknowledged for valuable suggestions for improvements to the article.

References

- [1] Z.G. Liu, J.T. Guo, L.L. Ye, G.S. Li, Z.Q. Hu, *Appl. Phys. Lett.* 65 (1994) 2666–2668.
- [2] G.B. Schaffer, J.S. Forrester, *J. Mater. Sci.* 32 (1997) 3157–3162.
- [3] N.Q. Wu, S. Lin, J.M. Wu, Z.Z. Li, *Mater. Sci. Technol.* 14 (1998) 287–291.
- [4] Z. Xinkun, Z. Kunyu, C. Baochang, L. Qiushi, Z. Xiuqin, C. Tiel, S. Yunsheng, *Mater. Sci. Eng. C* 16 (2001) 103–105.
- [5] C. Deidda, S. Doppiu, M. Monagheddu, G. Cocco, *J. Metastable Nanocryst. Mater.* 15/16 (2003) 215–220.
- [6] L. Takacs, *J. Solid State Chem.* 125 (1996) 75–84.
- [7] B.K. Yen, T. Aizawa, J. Kihara, *J. Am. Ceram. Soc.* 81 (1998) 1953–1956.
- [8] M. Puttaswamy, Y. Chen, B. Jar, J.S. Williams, *Mater. Sci. Forum* 312–314 (1999) 79–84.
- [9] G.B. Schaffer, P.G. McCormick, *Metall. Transact. A* 23A (1992) 1285–1290.
- [10] M. Mingliang, L. Xinkuan, X. Shenqui, C. Donglang, Z. Jingen, *J. Mater. Process. Technol.* 116 (2001) 124–127.
- [11] R. Koc, C. Meng, G.A. Swift, *J. Mater. Sci.* 35 (2000) 3131–3141.
- [12] M.S. El-Eskandarany, T.J. Konno, K. Sumiyama, K. Suzuki, *Mater. Sci. Eng. A: Struct. Mater.: Properties, Microstruct. Process. A* 217/218 (1996) 265–268.
- [13] M.S. El-Eskandarany, *Metall. Mater. Transact. A: Phys. Metall. Mater. Sci.* 27A (1996) 2374–2382.
- [14] M.S. El-Eskandarany, *J. Alloys Compd.* 305 (2000) 225–238.
- [15] L.L. Ye, M.X. Quan, *Nanostruct. Mater.* 5 (1995) 25–31.
- [16] K. Kudaka, I. Kiyokata, T. Sasaki, *J. Ceram. Soc. Jpn.* 107 (1999) 1019–1024.
- [17] M.V. Klein, J.A. Holy, W.S. Williams, *Phys. Rev. B* 17 (1978) 1546–1556.
- [18] M. Amer, M.W. Barsoum, T. El-Raghy, I. Weiss, S. Leclair, D. Liptak, *J. Appl. Phys.* 84 (1998) 5817–5819.